Length-Scale Dependence of the Superconductor-to-Insulator Quantum Phase Transition in One Dimension

Edmond Chow* and Per Delsing
Department of Microelectronics and Nanoscience, Chalmers University of Technology and Göteborg University, S-412 96, Göteborg, Sweden

David B. Haviland
Department of Physics, Royal Institute of Technology, S-100 44 Stockholm, Sweden
(Received 16 September 1997)

One-dimensional (1D) arrays of small-capacitance Josephson junctions demonstrate a sharp transition, from Josephson-like behavior to the Coulomb blockade of Cooper-pair tunneling, as the effective Josephson coupling between nearest neighbors is tuned with an externally applied magnetic field. Comparing the zero-bias resistance of three arrays with 255, 127, and 63 junctions, we observe a critical behavior where the resistance, extrapolated to $T = 0$, is independent of length at a critical magnetic field. Comparison is made with a theory of this $T = 0$ quantum phase transition, which maps to the 2D classical XY model. [S0031-9007(98)06542-9]

PACS numbers: 73.40.Gk, 73.23.Hk, 74.50.+r

The superconductor-to-insulator (SI) transition is an archetypical example of a quantum phase transition [1]. The Josephson junction (JJ) array is an ideal system for the study of this transition, because its fabrication is well controlled, and the array parameters can be accurately determined and directly related to the theoretical models. We present the first experimental measurements of the SI transition in 1D arrays of small-capacitance Josephson junctions. Our experiments directly demonstrate how measured transport quantities, which are determined by quantum fluctuations, have a diverging length dependence at the quantum critical point.

The SI transition has been extensively studied in 2D: Experiments have been carried out on granular [2–4] and homogeneous [5,6] thin films. Theoretical studies of the 2D case have concentrated on modeling the films as 2D arrays of small capacitance Josephson junctions (some recent references are [7–12]). Experiments with such arrays have been carried out [13,14]. Less extensively studied is the SI transition in 1D JJ arrays, where theory has been done [1,8,15–19] and is currently of active interest. Experiments with 1D systems have been carried out on long and narrow thin films of both granular [20] and homogeneous [21] composition. In contrast to thin films, the 1D JJ array can be made with a high degree of uniformity, and the parameters of interest in the theory can be directly and independently measured. Furthermore, we can design and fabricate a quasi-1D JJ array in such a way that we tune *in situ* the ratio of the Josephson coupling energy to the charging energy, which is the critical parameter in the theory.

Several 1D JJ arrays with nominally identical junction parameters, but having a different number of junctions, N, could be fabricated simultaneously on one chip. A scanning electron micrograph of a section of an array is shown in Fig. 1. The fabrication of the arrays has been discussed in detail elsewhere [22]. The arrays were made of Al, with an Al_2O_3 tunnel barrier. Each of the Al electrodes in the series array is connected to its neighbors by two junctions in parallel, thus forming a superconducting quantum interference device (SQUID) between nearest neighbors. The SQUID geometry was used so that an external perpendicular magnetic field, B, could tune the effective Josephson coupling, E_J, between nearest neighbors, $E_J = E_{J0}|\cos \pi B A_{\text{loop}}/\Phi_0|$, where $A_{\text{loop}} = 0.12\ \mu\text{m}^2$ is the effective area of the SQUID loop. Because the geometrical inductance of the SQUID loop $L_0 \ll \Phi_0/2\pi I_{C0}$, an external magnetic field creates a phase shift so that

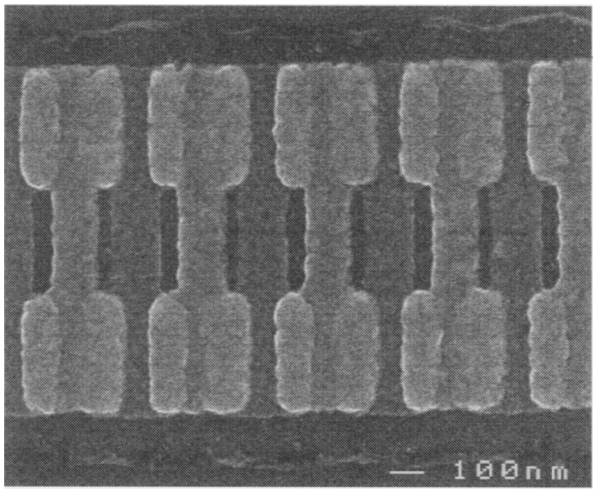

FIG. 1. A scanning electron micrograph of a section of the Josephson junction array. Tunnel junctions are formed at the overlap between the base electrode (darker gray) and the top electrode (lighter gray). The hole between neighboring electrodes forms the SQUID geometry.

 0031-9007/98/81(1)/204(4)$15.00

the critical current between nearest neighbors is modulated in a periodic way. Here, $E_{J0} = (\Phi_0/2\pi)I_{C0}$, where $\Phi_0 \equiv h/2e = 20.7\text{G}\ \mu\text{m}^2$ is the superconducting flux quantum, and $I_{C0} = \pi\Delta_0/2eR_T$ is the Ambegaokar-Baratoff critical current [23], which is calculated from the superconducting energy gap, Δ_0, and the junction normal tunnel resistance, R_T. In what follows, we will refer to the lumped SQUID as an effective junction with a tunable E_J, and a fixed charging energy $E_C = e^2/2C$, where C is the sum (parallel combination) of two junction capacitances.

The array resistance was found by taking the slope of the current-voltage (I-V) characteristic at high bias, $V > N(2\Delta_0/e)$, where $2\Delta_0 = 430\ \mu\text{eV}$ is the measured value of the gap for these $Al/Al_2O_3/Al$ tunnel junctions. This value of array resistance is consistent to within 0.2% with that value measured at lower bias, but at large magnetic fields, where superconductivity is completely suppressed. Dividing by N, we could calculate the normal state resistance per junction, R_T. The capacitance, $C = c_sA$, is determined from the junction area, A, which is measured from a scanning electron micrograph, and the specific capacitance, $c_S \simeq 45\ \text{fF}/\mu\text{m}^2$ [24].

Another important array parameter is the capacitance of each electrode to ground, C_0. The measurements described here were made on a sample with a Au ground plane located at a distance of 1.5 μm. By making the nearest neighbor capacitance relatively large, $C \simeq 3.5$ fF, and the spacing between electrodes relatively small (0.2 μm), we designed the arrays to have a large electrostatic screening length $\Lambda \equiv (C/C_0)^{1/2} \simeq 10$. When an excess charge is localized to one electrode, it will polarize the array over a distance 2Λ junctions. Having $\Lambda \gg 1$ should reduce the effects of disorder from random offset charges due to charge traps in the substrate, because any potential due to random offset charges should be averaged over this length scale.

Measurements were made in a dilution refrigerator. Special care was taken to filter the sample from high frequency electromagnetic radiation [22]. The preamplifier stage of our measurement scheme was specially designed to measure the high resistances associated with the Coulomb blockade [25]. The uniformity of the arrays could be estimated from the normal state resistance, which is found to be proportional to the number of junctions, with a maximum variation in R_T of $\pm 6\%$. For arrays with $E_J \gg E_C$ we observe the individual critical currents in the series array, which display a high degree of uniformity. Furthermore, the complete suppression of the Cooper pair current with magnetic field (see below), demonstrates that the two junctions of each SQUID are very nearly identical. In this paper, we discuss three arrays made on one chip, with a differing number of junctions; $N = 255$, 127, and 63. All three arrays had junction area $A \simeq 0.039\ \mu\text{m}^2$ and $R_T = 4.9\ \text{k}\Omega \pm 6\%$, from which we calculate $E_{J0}/E_C \simeq 142\ \mu\text{eV}/23\ \mu\text{eV} = 6.1$.

Figure 2a shows the I-V curve of the three arrays at zero magnetic field. The arrays are not truly superconducting, and there was actually a slope to the "zero-voltage" branch of the I-V curve, which gave a finite resistance. Furthermore, the observed "critical currents," i.e., first maximum of I vs V, occurring at $\simeq$0.03 mV, are only 1% of the classical Ambegaokar-Baratoff value. This critical current shows a clear dependence on array length: The longer the array, the larger I_C, indicating that superconducting behavior is favored in the longer array. As E_J was suppressed below E_{J0} with an externally applied magnetic field, the measured critical current of each array was reduced, and the resistance on the zero-voltage branch increased. Figure 2c shows the magnetic field dependence of I_C. In the neighborhood of $B_C = 58$ the curves in Fig. 2c cross one another so that for $B > B_C$, the longer the array, the smaller the critical current.

Figure 2b shows the I-V curve of the three arrays at a fixed magnetic field $B > B_C$. Here we see a new type of behavior which is dual to the $B < B_C$ behavior. The I-V curve is characterized by a zero current state for voltage below a threshold voltage, where the array switches to a finite current state. The threshold voltage increases as the magnetic field is increased, characteristic of the Coulomb blockade of Cooper pair tunneling (CBCPT). The magnetic field dependence of the threshold voltage

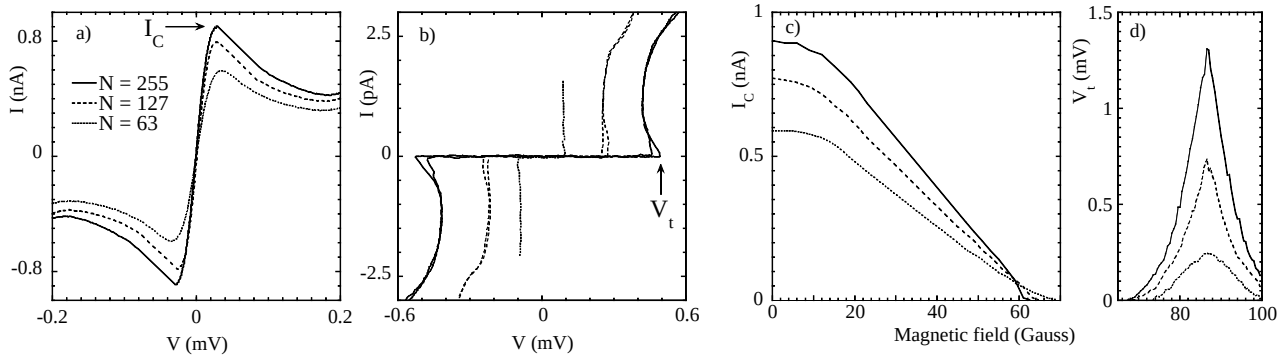

FIG. 2. Dependence of the I-V curves on array length, N, $T = 50$ mK. (a) The I-V curves at $B = 0$ G showing Josephson-like behavior and the critical current I_C. (b) The I-V curves at $B = 71$ G showing the Coulomb blockade of Cooper-pair tunneling and the threshold voltage V_t. (c) The magnetic field dependence of I_C. (d) The magnetic field dependence of V_t.

for $B > B_C$ is shown in Fig. 2d for the three arrays. We see that the longer the array, the larger the threshold voltage, indicating that insulating behavior is favored in the longer array.

Figures 2a–2d demonstrate how two quantities which characterize the nonlinearity of the I-V curve, I_C and V_T, depend on magnetic field and array length. We observe that in the longer array, superconducting behavior is favored (larger I_C) for $B < B_C$ and insulating behavior is favored (larger V_T) for $B > B_C$. In the neighborhood of B_C there is a dramatic change in the slope of the I-V curves at zero bias, as the arrays make a transition from Josephson-like behavior to the CBCPT. To probe this change in slope, we used a small amplitude, low-frequency (13 Hz) excitation to measure both the current $dI_{\rm rms}$ and voltage $dV_{\rm rms}$ by phase sensitive detection with two lock-in amplifiers. The excitation was then regulated so that the product $dI_{\rm rms}dV_{\rm rms}$ was held constant, around zero bias. The zero-bias resistance was taken to be $R_0 \equiv dV_{\rm rms}/dI_{\rm rms}$ for a fixed dissipation in the array of 10^{-16} W. This measurement technique allowed us to use an excitation just large enough for a detectable signal, while at the same time small enough so that we could probe the *linear* response of the array as it undergoes the transition. R_0 was thus measured as a function of temperature and magnetic field.

The temperature dependence of R_0 is shown in Fig. 3 for several values of the magnetic field for two arrays. Each set of curves (solid $N = 255$, dashed $N = 63$) shows qualitatively similar behavior: At zero magnetic field, we see that as each array is cooled, R_0 decreases to a value which is temperature independent. As the magnetic field is increased, the resistance of this flat tail increases, until it reaches a critical value, where $R_0(T)$ curves make a sharp turn to increasing resistance as the temperature goes to zero. Further increasing of the magnetic field drives the array into the insulating state, with a well defined zero current state below the threshold voltage.

A comparison of the two sets of curves in Fig. 3 reveals some very interesting and counterintuitive behavior. Concentrating on the bottom curve of each set ($B = 0$ for $N = 63$, dashed line, and $N = 255$, solid line), we find that the high temperature resistance is proportional to the array length. However, as the temperature is lowered, these two curves cross, and at low temperatures the resistance of the longer array is smaller than the shorter array. Comparing the sets of curves in Fig. 3 pairwise, we can follow how this crossover behavior evolves as E_J is tuned with magnetic field (open circles and dotted line in Fig. 3). Thus we can determine a $T = 0$ critical point, where the array resistance appears to be independent of length. This point, which is labeled J^* in Fig. 3 is the point where the $R_0(T)$ curves begin to turn upwards, indicating insulating behavior as $T \to 0$ in each array.

We can find explanation for this nonclassical dependence of R_0 on temperature and array length in the theory

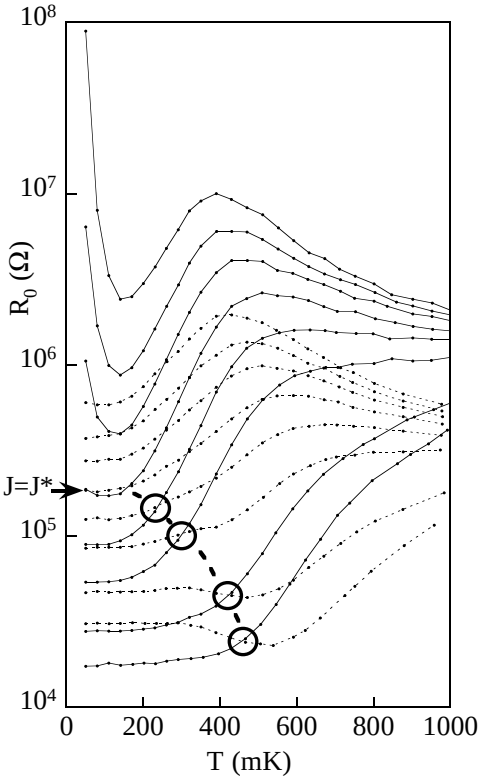

FIG. 3. Comparison of two arrays with $N = 255$ (solid line) and $N = 63$ (dashed line). $R_0(T)$ is measured at the same magnetic fields in each set of curves (from bottom to top $B = 0$, 27, 47, 53, 57, 60, 62, and 64 G). The crossing point is circled, where the resistance is the same for $N = 255$ and $N = 63$. As we approach the critical magnetic field, the temperature of this crossing point goes to zero (connected dotted line). At the critical point (labeled J^*) the $T = 0$ resistance is independent of array length.

of the quantum 1D JJ array. Theoretical treatment of the quantum 1D JJ array, where both the charging and coupling energy were included, has mapped this problem to the $(1 + 1)$D classical uniform XY model [1,15], the extra dimension being imaginary time, $i\hbar/k_BT$. The mapping could be carried out for a model where $C \ll C_0$ and the dimensionless coupling constant was found to be $(E_J/E_{C_0})^{1/2}$, where $E_{C_0} \equiv e^2/2C_0$. For our case, where $C \gg C_0$, the effective charging energy is presumably E_{C_0}/Λ, so that the dimensionless coupling constant is $J = (E_J/\Lambda E_C)^{1/2}$.

In this picture, quantum "phase slips," or finite voltage across the 1D array at zero temperature, correspond to the appearance of free vortices in the 2D XY model. Temperature enters into the picture by setting the finite size of the system in the imaginary time dimension. In a real experiment, finite size effects will play an important role. The temperature independent "flat tail" may result when we cool the real system so that the imaginary time dimension is larger, and the finite size in real space determines the energy for free vortex formation. Taking the resistance at the minimum temperature, $R_0(T_{\rm min})$ as

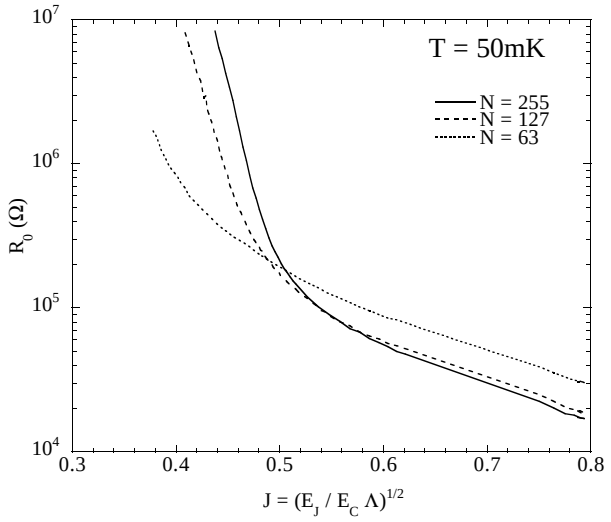

FIG. 4. The zero-bias resistance, $R_0(T_{\min})$, plotted versus the experimental value of the coupling constant, $J = [E_J(B)/\Lambda E_{C0}]^{1/2}$, at $T = 50$ mK. In the vicinity of $J = J^* \simeq 0.5$ the three curves cross one another. For $J < J^*$ (insulating side) R_0 increases as N increases. For $J > J^*$ (superconducting side) R_0 decreases as N increases.

being proportional to the probability for free vortex formation, one can argue that [26]

$$R_0(T_{\min}) \sim N^{2-\pi J}. \quad (1)$$

The power law results because the energy for vortex formation is logarithmic in the system size for the 2D XY model. At $J = J^* \equiv 2/\pi$, $R_0(T_{\min})$ is independent of N, and a transition occurs which becomes sharper as $N \to \infty$. For $J > J^*$, the measured $R_0(T_{\min})$ would actually be smaller for a larger array. This counterintuitive behavior arises because a larger system is more stable against quantum fluctuations. Precisely this behavior is observed when comparing the SI transition in these three arrays of different lengths (see Fig. 3 for comparison of $N = 255$ and $N = 63$).

Figure 4 shows R_0 taken at the lowest temperature, versus $J = (E_J/\Lambda E_C)^{1/2}$, which can be calculated from the magnetic field. The absolute magnitude of J has a large experimental uncertainty of about a factor of ± 2, primarily due to uncertainty in the values of Λ and E_C, which should nevertheless be the same for all three arrays. The observed value of $J^* \simeq 0.5$, where the three curves cross one another in Fig. 4, does compare well with the simple theoretical value of $2/\pi = 0.637$. However, the power law behavior predicted by Eq. (1) is not observed in the critical region. This may be due to the fact that (1) assumes a square array, and neglects the screening effects of bound vortex-antivortex pairs. Nevertheless, the mapping to a 2D XY model captures the basic transition, and its qualitative dependence on N.

We acknowledge S. M. Girvin for theoretical analysis, and helpful conversations with T. Claeson, M. Jonson, R. Shekhter, J. Kinaret, and S. Eggert. This work was supported by the Swedish NFR, TFR, the Swedish Nanometer Laboratory, and the Wallenberg Foundation.

*Current address: Sandia National Labs, Albuquerque, NM 87185.

[1] S. L. Sondhi, S. M. Girvin, J. P. Carini, and D. Shahar, Rev. Mod. Phys. **69**, 315 (1996).
[2] H. M. Jaeger, D. B. Haviland, B. G. Orr, and A. M. Goldman, Phys. Rev. B **40**, 182 (1989).
[3] R. P. Barber and R. C. Dynes, Phys. Rev. B **48**, 10 618 (1993).
[4] A. F. Hebard and M. A. Paalanen, Phys. Rev. Lett. **65**, 927 (1990).
[5] Y. Liu, D. B. Haviland, B. Nease, and A. M. Goldman, Phys. Rev. B **47**, 5931 (1993).
[6] J. M. Valles, R. C. Dynes, and J. P. Garno, Phys. Rev. Lett. **69**, 3567 (1992).
[7] E. Granato and J. M. Kosterlitz, Phys. Rev. Lett. **65**, 1267 (1990).
[8] M. C. Cha *et al.*, Phys. Rev. B **44**, 6883 (1991).
[9] A. P. Kampf and G. T. Zimanyi, Phys. Rev. B **47**, 279 (1993).
[10] E. Šimánek, Phys. Lett. A **177**, 367 (1993).
[11] A. van Otterlo, K. H. Wagenblast, R. Fazio, and G. Schön, Phys. Rev. B **48**, 3316 (1993).
[12] M. Wallin, E. S. Sorensen, S. M. Girvin, and A. P. Young, Phys. Rev. B **49**, 12 115 (1994).
[13] H. S. J. van der Zant *et al.*, Phys. Rev. Lett. **69**, 2971 (1992).
[14] C. D. Chen *et al.*, Phys. Rev. B **51**, 15 645 (1995).
[15] R. M. Bradley and S. Doniach, Phys. Rev. B **30**, 1138 (1984).
[16] S. E. Korshunov, Euro. Phys. Lett. **9**, 107 (1989).
[17] P. A. Bobbert, R. Fazio, G. Schön, and A. D. Ziakin, Phys. Rev. B **45**, 2294 (1992).
[18] L. I. Glazman and A. I. Larkin, Phys. Rev. Lett. **79**, 3736 (1997).
[19] A. A. Odintsov, Phys. Rev. B **54**, 1228 (1996).
[20] A. V. Herzog, P. Xiong, F. Sharifi, and R. C. Dynes, Phys. Rev. Lett. **76**, 668 (1996).
[21] F. Sharifi, A. V. Herzog, and R. C. Dynes, Phys. Rev. Lett. **71**, 428 (1993).
[22] D. B. Haviland, S. H. M. Persson, P. Delsing, and C. D. Chen, J. Vac. Sci. Technol. **13**, 1839 (1996).
[23] V. Ambegaokar and A. Baratoff, Phys. Rev. Lett. **10**, 486 (1963); **11**, 104(E) (1963).
[24] P. Delsing, T. Claeson, K. K. Likharev, and L. S. Kuzmin, Phys. Rev. B **42**, 7439 (1990).
[25] P. Delsing, Ph.D. thesis, Chalmers University of Technology, Göteborg, 1990, ISBN No. 91-7032-509-x.
[26] S. M. Girvin (private communication).